arXiv:cond-mat/0008089v3 [cond-mat.stat-mech] 8 Apr 2005

Beyond the Wigner Distribution: Schrödinger Equations and Terrace Width Distributions

Howard L. Richards[1, 2, *] and T. L. Einstein[1, †]

[1] *Department of Physics, University of Maryland, College Park, MD 20742-4111*
[2] *Department of Physics, Texas A & M University–Commerce, Commerce, TX 75429-3011*

(Dated: April 7, 2005)

The so-called generalized Wigner distribution has earlier been shown to be an excellent approximation for the terrace width distribution (TWD) of vicinal surfaces characterized by step-step interactions that are perpendicular to the average step direction and fall off as the inverse square of the step spacing. In this paper we show that the generalized Wigner distribution can be derived from a plausible, phenomenological model in which two steps interact with each other directly and with other steps through a position-dependent pressure. We also discuss generalizations to more general step-step interactions and show that the predictions are in good agreement with TWDs derived from numerical transfer-matrix calculations and Monte Carlo simulations. This phenomenological approach allows the step-step interaction to be extracted from experimental TWDs.

PACS numbers: 05.40.-a 68.35.Md 05.70.Np, 02.50.-r,

I. INTRODUCTION

Vicinal surfaces consist of terraces divided by steps which interact with each other via a variety of mechanisms, including elastic, dipolar, and indirect electronic interactions. Since these interactions directly determine the distribution of terrace widths, the use of terrace width distributions (TWDs) to determine the step-step interactions is an important goal. Theoretical attempts towards this goal have produced differing results depending upon specific approximations [1, 2, 3, 4, 5, 6, 7].

In many cases, the potential energy V due to the interaction between neighboring steps can be written in terms of the distance L between the steps as

$$V(L) = \frac{A}{L^2}\,. \tag{1}$$

This model of interacting steps can be mapped directly onto the Calogero-Sutherland model [8, 9] of interacting spinless fermions (or hard-core bosons) in one spatial dimension (Fig. 1); in this picture, the direction along the steps (the y-direction in "Maryland notation") is interpreted as time, and the steps themselves are interpreted as the world-lines of the spinless fermions. The static properties of this system (such as the TWD) depend on A only through the dimensionless interaction strength

$$\tilde{A} \equiv \frac{\tilde{\beta} A}{(k_{\rm B}T)^2}\,, \tag{2}$$

where $\tilde{\beta}$ is the step stiffness, $k_{\rm B}$ is Boltzmann's constant, and T is the absolute temperature. The TWD can be calculated exactly [8, 9] when $\tilde{A} = -1/4$, 0, or 2.

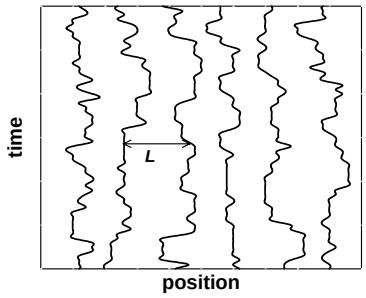

FIG. 1: Steps on a vicinal surface can be mapped to the worldlines of spinless fermions or hard-core bosons in one spatial dimension (the x-direction). The "time" axis corresponds to the y-axis on the vicinal surface.

An argument [10] from random matrix theory originally due to Wigner suggests that these three exact TWDs can be approximated by

$$P(s) = a_\varrho s^\varrho \exp(-b_\varrho s^2)\,, \tag{3}$$

where $s \equiv L/\langle L\rangle$, the constraint $\langle s\rangle = 1$ gives b_ϱ [see Eq. (32)], a_ϱ is a normalization constant, and the relationship between $\tilde{A}$ and ϱ is [8, 9]

$$\tilde{A} = \frac{\varrho}{2}\left(\frac{\varrho}{2} - 1\right)\,. \tag{4}$$

These "Wigner distributions" have proven quite successful and have been widely used [11, 12, 13] in nuclear physics (in which case s is the spacing between energy levels), random matrix theory, quantum transport, and universal conductance fluctuations. There have been a number of attempts [14, 15, 16, 17, 18, 19, 20] to interpolate between these three special cases.

*Corresponding author: Howard˙Richards@tamu-commerce.edu; http://faculty.tamu-commerce.edu/HRichards/index.html
†einstein@umd.edu; http://www2.physics.umd.edu/~einstein/

The so-called generalized Wigner distribution [21] is defined by the simple assumption that Eq. (3) and Eq. (4) remain valid for all values of $\tilde{A}$. (This is only reasonable for positive or weakly negative values of $\tilde{A}$ [22].) The generalized Wigner distribution appears to be in better agreement with computer simulations of vicinal surfaces [23] than its competitors, and is in reasonable agreement with many experimental TWDs [25]. Furthermore, it has been proved that for rational values of ϱ, $P(s) \propto s^{\varrho}$ as $s \to 0$ [26, 27, 28]. However, for arbitrary values of $\tilde{A}$ there is no clear relation between random matrix theory and the Calogero-Sutherland model. This paper provides a formal and physically intuitive justification for Eq. (3) for arbitrary values of $\tilde{A}$; the resulting formalism allows us to consider more general step-step interactions than Eq. (1). Some of these results have been mentioned briefly elsewhere [23] but are explained here in detail.

The organization of this paper is as follows. In Sec. II, we show that the generalized Wigner distribution can be derived from a phenomenological model, which reduces, under certain circumstances, to the two-particle Calogero model [8]. This leads, by separation of variables, to a one-variable Schrödinger equation that determines the TWD. We extend this treatment to non-trivial examples in Sec. III. The significant process of extracting step-step interactions from experimental TWDs is discussed in Sec. IV. Finally, we conclude in Sec. V with some possible extensions of this work.

II. PHYSICAL EXPLANATION OF THE GENERALIZED WIGNER DISTRIBUTION

A. Deriving a Schrödinger equation from the generalized Wigner Distribution

Given a system of steps with interactions of the form specified by Eq. (1) and a TWD given by the corresponding generalized Wigner distribution [Eq. (3)], we can define a wave function such that $\psi_0^2(s) \equiv P(s)$:

$$\psi_0(s) = a_{\varrho}^{1/2} s^{\varrho/2} \exp(-b_{\varrho} s^2/2)\,. \tag{5}$$

Differentiating twice, we find

$$\begin{aligned} \frac{\mathrm{d}^2}{\mathrm{d}s^2}\psi_0(s) &= \left[\frac{\varrho}{2}\left(\frac{\varrho}{2}-1\right)s^{-2} - (\varrho+1)b_{\varrho} + b_{\varrho}^2 s^2\right]\psi_0(s) \\ &= \left[\tilde{A}s^{-2} - (\varrho+1)b_{\varrho} + b_{\varrho}^2 s^2\right]\psi_0(s)\,, \end{aligned} \tag{6}$$

where we have used Eq. (4). Eq. (6) allows us, in somewhat the same spirit as the Gruber-Mullins approximation [1], to propose the following dimensionless Schrödinger equation:

$$\frac{\mathrm{d}^2}{\mathrm{d}s^2}\psi_n(s) = [\tilde{U}(s) + \tilde{V}(s) - \tilde{E}_n]\psi(s)\,, \tag{7}$$

where

$$\tilde{V}(s) = \tilde{A}s^{-2} \tag{8}$$

is the explicit step-step interaction potential in dimensionless form and

$$\tilde{U}(s) = b_{\varrho}^2 s^2 \tag{9}$$

is a dimensionless potential due to other steps not explicitly considered. (This idea is explained in the next subsection.) By inspection we see that $\psi_0(s)$ is the ground state wave function (it has only one antinode), with an eigenvalue given by

$$\tilde{E}_0 = (\varrho+1)b_{\varrho}\,. \tag{10}$$

In comparing different experimental TWDs with a range of values of $\langle L\rangle$ but with presumably the same step-step interaction $V(L)$, it is often useful to rewrite Eq. (7) in its dimensional form

$$\frac{(k_{\mathrm{B}}T)^2}{\tilde{\beta}}\frac{\mathrm{d}^2}{\mathrm{d}L^2}\Psi_n(L) = [U(L) + V(L) - E_n]\Psi_n(L)\,, \tag{11}$$

where $V(L)$ is given by Eq. (1),

$$U(L) \equiv \frac{(k_{\mathrm{B}}T)^2}{\tilde{\beta}\langle L\rangle^2}\tilde{U}\left(\frac{L}{\langle L\rangle}\right) \tag{12}$$

and

$$E_n \equiv \frac{(k_{\mathrm{B}}T)^2}{\tilde{\beta}\langle L\rangle^2}\tilde{E}_n. \tag{13}$$

Throughout this paper we will alternate freely and without comment between dimensional and dimensionless representations.

Eq. (7) can be solved for all the eigenfunctions and eigenvectors [29], so one can conveniently consider perturbations from the purely inverse-square interaction given by Eq. (1). The eigenfunctions are

$$\psi_n(s) = c_n s^{\varrho/2}\exp\left(-b_{\varrho}s^2\right)\,{}_1F_1\left(-n, \frac{\varrho+1}{2}, b_{\varrho}s^2\right)\,, \tag{14}$$

where n is any nonnegative integer, c_n is a normalization constant, and ${}_1F_1(a,b,x)$ is Kummer's confluent hypergeometric function [30]. The corresponding eigenvalues are

$$\tilde{E}_n = (\varrho+1+4n)b_{\varrho}\,. \tag{15}$$

B. Deriving the generalized Wigner Distribution from a Schrödinger equation

An undesirable element of the previous derivation was that it implicitly required that one of the steps be held fixed, which introduced an artificial (and unnecessary) difference between steps. Furthermore, the quadratic nature of $\tilde{U}(s)$ was not well explained. In this subsection we explore these issues.

The Calogero-Sutherland [8, 9] model with an infinite number of interacting spinless fermions would be an ideal model of the vicinal surface, but as mentioned above, it is only integrable for three values of $\tilde{A}$. A useful alternative is to consider only two adjacent fermions explicitly and model the effects of the other fermions phenomenologically through the pressure they exert, yielding the Hamiltonian

$$\mathcal{H} = -\frac{1}{2}\left(\frac{\partial^2}{\partial x_1^2}+\frac{\partial^2}{\partial x_2^2}\right)+\tilde{V}(x_2-x_1)-x_1\mathcal{P}_1(x_1)+x_2\mathcal{P}_2(x_2)\,. \tag{16}$$

Here $\mathcal{P}_i$ is the pressure exerted on fermion i, which we allow to be position-dependent because the limited correlation length in the x-direction leads to an effectively finite system size [31]. Accordingly, we place the $\mathcal{V}$ fermions immediately to the left of fermion 1 in a "box" with a fixed left wall at $x=-\mathcal{V}$; the right wall is at x_1, the position of fermion 1. The volume (length) of this box is $\mathcal{V}_1=\mathcal{V}+x_1$. The pressure $\mathcal{P}_1$ can be expanded as follows:

$$\begin{aligned}\mathcal{P}_1(x_1) &= \mathcal{P}+x_1\left(\frac{\partial\mathcal{P}_1}{\partial x_1}\right)\Big|_{x_1=0}+\mathcal{O}(x_1^2) &(17)\\ &= \mathcal{P}+x_1\left(\frac{\partial\mathcal{P}_1}{\partial\mathcal{V}_1}\right)\Big|_{\mathcal{V}_1=\mathcal{V}}+\mathcal{O}(x_1^2) &(18)\\ &= \mathcal{P}-x_1(\mathcal{V}\kappa)^{-1}+\mathcal{O}(x_1^2)\,, &(19)\end{aligned}$$

where $\mathcal{P}\equiv\mathcal{P}_1(0)$ and the compressibility κ is given by

$$\kappa\equiv-\frac{1}{\mathcal{V}}\left(\frac{\partial\mathcal{P}_1}{\partial\mathcal{V}_1}\right)^{-1}\Big|_{\mathcal{V}_1=\mathcal{V}}\,. \tag{20}$$

Likewise, we place the $\mathcal{V}$ fermions immediately to the right of fermion 2 in a "box" of volume (length) $\mathcal{V}_2=\mathcal{V}-x_2$, yielding

$$\mathcal{P}_2(x_2)=\mathcal{P}+x_2(\mathcal{V}\kappa)^{-1}+\mathcal{O}(x_22)\,. \tag{21}$$

Combining Eqs. (16), (19), and (21), we obtain

$$\begin{aligned}\mathcal{H} &= -\frac{1}{2}\left(\frac{\partial^2}{\partial x_1^2}+\frac{\partial^2}{\partial x_2^2}\right)+\tilde{V}(x_2-x_1)+(x_2-x_1)\mathcal{P}\\ &\quad+(x_1^2+x_2^2)(\mathcal{V}\kappa)^{-1}+\mathcal{O}(x_2^3-x_1^3)\,. &(22)\end{aligned}$$

Finally, we can make the following change of variables:

$$\begin{aligned}x_{\rm cm} &= \frac{x_1+x_2}{2} &(23)\\ s &= x_2-x_1\geq 0\,. &(24)\end{aligned}$$

This allows us to rewrite the Hamiltonian as follows:

$$\begin{aligned}\mathcal{H} &= -\left(\frac{1}{4}\frac{\partial^2}{\partial x_{\rm cm}^2}+\frac{\partial^2}{\partial s^2}\right)+\tilde{V}(s)\\ &\quad+[\mathcal{P}s+(\mathcal{V}\kappa)^{-1}s^2]+4(\mathcal{V}\kappa)^{-1}x_{\rm cm}^2+\mathcal{O}(sx) &(25)\end{aligned}$$

If terms of quadratic and higher order in Eqs. (19) and (21) can be neglected, the Hamiltonian can be separated into a part that depends only on s and a part that depends only on $x_{\rm cm}$:

$$\mathcal{H}=\mathcal{H}_{\rm cm}+\mathcal{H}_s\,, \tag{26}$$

where

$$\mathcal{H}_{\rm cm}=-\frac{1}{4}\frac{\partial^2}{\partial x_{\rm cm}^2}+4(\mathcal{V}\kappa)^{-1}x_{\rm cm}^2 \tag{27}$$

and

$$\mathcal{H}_s=-\frac{\partial^2}{\partial s^2}+\tilde{V}(s)+\tilde{U}(s) \tag{28}$$

with

$$\tilde{U}(s)=\mathcal{P}s+(\mathcal{V}\kappa)^{-1}s^2\,. \tag{29}$$

None of the argument so far requires the assumption that $\tilde{V}(s)$ is given by Eq. (8). In the next section we will examine how well this phenomenological formalism works when applied to other forms of $\tilde{V}(s)$.

If $(\mathcal{V}\kappa)^{-1}\gg\mathcal{P}$, we can neglect the term $\mathcal{P}s$ in $\tilde{U}(s)$. The resulting Hamiltonian $\mathcal{H}$ can easily be seen to be the Hamiltonian of the two-fermion Calogero model [8],

$$\mathcal{H}=-\left(\frac{\partial^2}{\partial x_1^2}+\frac{\partial^2}{\partial x_2^2}\right)+\tilde{V}(x_2-x_1)+(x_1^2+x_2^2)\omega^2\,, \tag{30}$$

where we identify from Eq. (9)

$$\omega^2=(\mathcal{V}\kappa)^{-1}\,. \tag{31}$$

More importantly, with the identification

$$\omega=b_\varrho\equiv\left[\frac{\Gamma\left(\frac{\varrho+2}{2}\right)}{\Gamma\left(\frac{\varrho+1}{2}\right)}\right]^2\,, \tag{32}$$

which again comes from the constraint $\langle s\rangle=1$, we see that

$$(\mathcal{H}_s-\tilde{E}_n)\psi_n(s)=0 \tag{33}$$

is just Eq. (7) and again leads to the generalized Wigner distribution.

Finally, it should be pointed out that the one particle "Calogero model," with a Hamiltonian given by

$$\mathcal{H}=-\frac{{\rm d}^2}{{\rm d}x^2}+x^2\omega^2\,, \tag{34}$$

is really what in essence is used in the many Gaussian approximations [1, 2, 3, 4, 5, 6, 7]. These approximations, however, produce conflicting functional relationships between ω and $\tilde{A}$. This is hardly surprising, since $\tilde{V}$ does not appear explicitly in Eq. (34). By using a two-particle Calogero model, we are able to state unambiguously the relationship between ω and $\tilde{A}$.

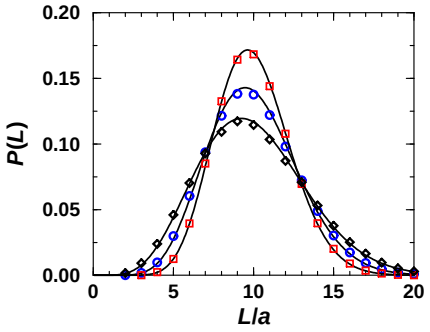

FIG. 2: [Color online] TWDs for systems of steps with step-step interactions of the form $\tilde{V}(s) = \tilde{A}_3 s^{-3}$. Diamonds, circles, and squares mark TWDs from Monte Carlo simulations with $\tilde{A}_3 = 0.5$, 2, and 6, respectively. Solid lines are solutions of Eq. (7) for the same values of $\tilde{A}_3$ and with $\tilde{U}(s) \propto s^2$.

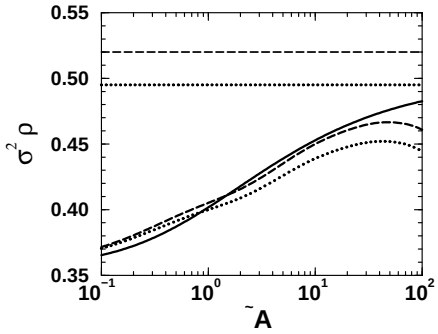

FIG. 3: Comparison of $\sigma^2\varrho$ from the generalized Wigner distribution (solid curve) and transfer-matrix calculations for nearest-neighbor-only (NN) interactions (dashed curve) and interactions out to next-nearest neighbors (NNN) (dotted curve). The transfer-matrix calculations were performed with 5 steps, $\langle L \rangle = 5$, $\tilde{V}(s)$ given by Eq. (8), and $k_B T = 0.84\epsilon$, where ϵ is the energy of a single kink. It appears that the nearest-neighbor-only interactions are in better agreement with the generalized Wigner distribution, although this judgment is hampered by the small system size and the breakdown, at large $\tilde{A}$, of the continuum step model. The dashed and dotted lines indicate limits of $\sigma^2\varrho$ for NN and NNN interactions, respectively, as derived from Gaussian approximations of the the continuum step model in the limit of large $\tilde{A}$ [3, 4].

III. NONTRIVIAL EXTENSIONS

Here and in the remainder of the text, for our numerical work we use models that are discrete in both the y-direction and the x-direction [2, 5, 7, 32], in contrast to the continuum step mode, which corresponds to the description given above. Specifically, in Monte Carlo simulations we use the terrace-step-kink (TSK) model, in which the kinks can be any integral number of lattice units long. Our transfer-matrix calculations use the restricted TSK model, in which the kinks can only be of one lattice unit. In both models there are exact expressions for the stiffness of an isolated step as a function of temperature [32]. The interaction between steps is given by a specified function $V(L)$, as with the continuum step model. Further details of our numerical work can be found in Refs. 23, 24.

Eq. (7) can be extended to step-step interactions of forms other than Eq. (8). In this section we will present a few arbitrary but physically motivated step-step interactions and show that the phenomenological method of the preceding section still yield TWDs in excellent agreement with numerical simulations of the TSK model.

As a first example, we consider interactions of the form

$$\tilde{V}(s) = \tilde{A}_3 s^{-3} \,, \tag{35}$$

which would be a plausible subdominant term in a Taylor expansion of the step-step interaction in s^{-1}. Figure 2 shows TWDs obtained by Monte Carlo simulations of steps interacting with this potential for three different values of $\tilde{A}_3$. Since the Wigner distribution worked so well with nearest-neighbor interactions of the form given by Eq. (8), we again take $\tilde{U}(s) \propto s^2$. The solutions of the Schrödinger equation are in excellent agreement with the Monte Carlo data.

Interestingly, when *all* steps interact (via the potential given by Eq. (8), the variance of a TWD with a fixed value of $\tilde{A}$ will be smaller than the variance of a TWD with the same value of $\tilde{A}$ and just nearest-neighbor steps interacting. Numerical evidence supports this intuition, and in fact it appears that the Wigner distribution describes TWDs from nearest-neighbor interactions better than TWDs from all steps interacting (see Fig. 3). On the other hand, the phenomenological approach which leads to the generalized Wigner distribution depends only on the interaction between nearest neighbor steps, which is identical in both cases.

The difference appears to come from terms in Eq. (25) that are neglected in Eq. (30). Since the variance is decreased by interactions with more steps, it is clear that increasing the number of interacting steps will not increase the linear term $\mathcal{P}$ in Eq. (25) — that would increase the variance. Instead, it appears that increasing the number of interacting steps increases the quadratic terms in Eqs. (19) and (21). This would decrease the variance and correspond to the intuitive notion that the steps "interact more strongly" while still observing the constraint $\langle s \rangle = 1$. Unfortunately, it also destroys the separability of the Schrödinger equation.

A variety of circumstances, such as the presence of adsorbates [33] or electronic surface states [34, 35], can give rise to short-ranged attractive forces between steps, oscillating step-step interaction potentials, and other complicated interactions. Under such circumstances, one

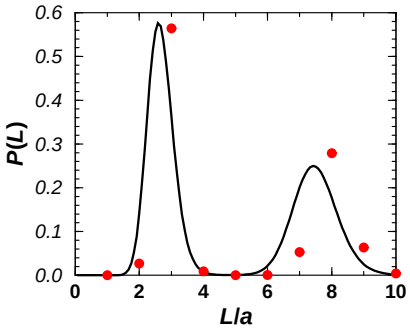

FIG. 4: [Color online] A transfer-matrix calculation (•) of the TWD for a system of five steps with a mean step separation of 5 lattice units and the oscillating step-step potential given by Eq. (37). The curve is the solution of the corresponding Schrödinger equation and contains no free parameters.

typically finds terraces of two more-or-less well-defined widths; interactions with steps beyond nearest neighbors can segregate these widths, leading to "step bunching" [36]. This situation is somewhat analogous to liquid-gas coexistence, and as with liquid-gas coexistence the compressibility diverges. As a result, $\tilde{U}(s)$ is linear in s [Eq. (29)].

Vicinal surfaces with both elastic and surface-state mediated electronic interactions may be characterized by potentials of the form [34, 35]

$$V(L) = AL^{-2} + BL^{-3/2}\cos(2k_F L + \phi)\,, \qquad (36)$$

where A is determined by the elastic interactions, B is determined by the coupling to the surface state, k_F is the Fermi energy, and ϕ is a phase shift. The oscillations of this potential can give rise to a coexistence as described above, together with a diverging compressibility and a linear $U(L)$. As a dramatic — albeit rather unphysical — example, in Fig. 4 we compare transfer-matrix TWDs derived from the corrugated interaction potential

$$\tilde{V}(s) = 4\cos(2\pi s) \qquad (37)$$

[a special case of Eq. (36)] with corresponding solutions of Eq. (7). Since the TWDs now have multiple peaks, clearly neither the generalized Wigner distribution nor a Gaussian distribution is appropriate. Again, considering that there are no free parameters, the phenomenological TWD is in excellent agreement with the transfer-matrix TWD. The slight disagreement is probably due to finite-size effects in the transfer-matrix calculation (which involved only five steps with $\langle L\rangle = 5$).

IV. SOLVING FOR THE STEP-STEP INTERACTION

The chief practical interest in terrace width distributions comes from a desire to use experimental data to determine the interaction potential $V(L)$, or equivalently $\tilde{V}(s)$. In this section we discuss three progressively more sophisticated methods. The first two are appealing in their simplicity, but they suffer from serious flaws, and therefore should be avoided. By building on them, we introduce the third method, which is more computationally intensive than the preceding two, but which has the flexibility necessary to be appplied to real experimental data. For more details see Ref. 37.

A. Naive direct numerical approach

In Sec. II, we derived a Schrödinger equation that included $\tilde{V}(s)$ in an obvious way, and in Sec. III we have seen that similar Schrödinger equations yield TWDs for more complicated interactions that are in excellent agreement with numerical simulations of the TSK model. It is tempting to follow an analogous path when dealing with experimental data, using the following procedure:

1. Connect the experimental data points with a smooth interpolating function $P(s)$, such as a cubic spline.
2. Calculate $\psi(s) \equiv \sqrt{P(s)}$.
3. Find $\mathrm{d}^2\psi/\mathrm{d}s^2$.
4. The total potential is $\tilde{V}(s) + \tilde{U(s)} - E \equiv [\psi(s)]^{-1}[\mathrm{d}^2\psi(s)/\mathrm{d}s^2]$.
5. At large s, $\tilde{V}(s)$ is negligible, so the total is given by $\tilde{U}(s) - E$, which should be constant plus either a quadratic function of s or a linear function of s.
6. Subtract $\tilde{U}(s) - E$ from the potential to recover the step-step interaction $\tilde{V}(s)$.

This method has two serious problems. Experimental TWDs will contain measurements indicating $P(s) = 0$, which lead to division by zero in determining the total potential. Furthermore, typical statistical fluctuations make the numerical estimates of $\mathrm{d}^2\psi/\mathrm{d}s^2$ from experimental data extremely unreliable.

B. Fitting the TWD to a preconceived form of $P(s)$

One may eliminate both of these problems by first performing a least-squares fit of the TWD to some positive definite and twice-differentiable function. For example, one might use

$$P(s) = c_0 s^{\varrho}(1 + c_1 s + c_2 s^2)\exp(-bs^2)\,, \qquad (38)$$

where c_0 is a normalization constant and c_1, c_2, ϱ, and b all are parameters to be fitted. The fitted $P(s)$ can then be analyzed as above.

The shortcomings of this second approach are more subtle. Eq. (38), for example, will always yield a potential that diverges as s^{-2} as s approaches zero. In fact, we have fitted Eq. (38) to the Monte Carlo data shown in Fig. 2. Instead of correctly reproducing the potential $\tilde{V}(s) = \tilde{A}_3 s^{-3}$, the analysis of the fitted $P(s)$ produced an interaction that is well approximated by $\tilde{V}(s) \approx \tilde{A}_2 s^{-2}$. The intersection of this derived potential with the known, true potential is for a value of L near $\langle L \rangle$, which is not surprising — the TWD contains more information about the interaction where $P(s)$ is large.

C. Recommended: Fitting the interaction $V(L)$ to a preconceived form

The method we *do* recommend is more computationally demanding, but it suffers from none of the above defects:

1. Parameterize $V(L)$, and make a crude initial estimate of the values of the parameters. At least some information on the form of the interaction is often available — whether it is influenced by a surface electronic state, for example. In principle, $U(L)$ contains a term linear in L and a term quadratic in L, as in Eq. (29); in practice, one can often use either a purely quadratic form of $U(L)$ (as was done to derive the generalized Wigner distribution) or a purely linear form of $U(L)$ (if the compressibility diverges).

2. Solve Eq. (11) numerically for the specified parameters to find $\Psi_0(L)$.

3. Find

$$\chi^2 = \sum_L \left[\Psi_0^2(L) - P_{\rm exp}(L)\right]^2 \qquad (39)$$

for this set of parameters, where $P_{\rm exp}(L)$ is the experimental TWD.

4. Iterate procedural steps 2 and 3 in a minimization routine to find parameters for which $\Psi_0^2(L)$ best fits the experimental TWD.

TABLE I: Parameters in Eq. (40) determined by a least-squares fit of the phenomenological TWD to the Monte Carlo TWD (see Fig. 5).

	$\tilde{A}_1$	$\tilde{A}_2$	$\tilde{A}_3$	$\tilde{A}_4$
true	0	0	2	0
fit	6.862	1.1035	0.40164	0.05215

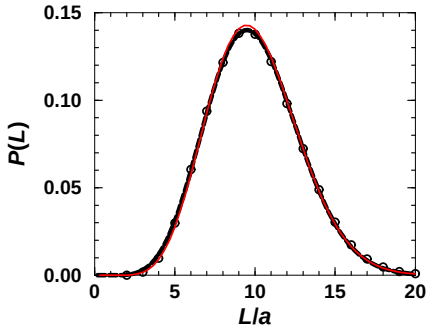

FIG. 5: [Color online] Monte Carlo (○) and phenomenological (solid curve) TWDs for steps interacting with a potential $\tilde{V}(s) = 2s^{-3}$. The dashed curve shows a least squares fit using a potential of the form given in Eq. (40).

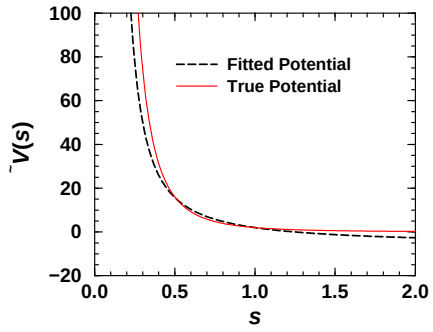

FIG. 6: [Color online] The solid curve shows the step-step interaction actually used (solid curve) to generate the Monte Carlo TWD shown in Fig. 5. The dashed curve shows the step-step interaction of the form given by Eq. (40) with the parameters given in Table I, which were determined by a least-squares fit of the phenomenological TWD to the Monte Carlo TWD. To facilitate a better comparison, the fitted potential has been shifted by a constant energy so that it coincides with the true potential at $s = 1$.

In Fig. 6 we apply this approach to the Monte Carlo TWD shown in Fig. 5. We parameterize $\tilde{V}(s)$ by

$$\tilde{V}(s) = \tilde{A}_1 s^{-1} + \tilde{A}_2 s^{-2} + \tilde{A}_3 s^{-3} + \tilde{A}_4 s^{-4}\,; \qquad (40)$$

this form amounts to a generalization of the two-parameter fit discussed in Ref. 38, where the only allowed term in $\tilde{V}(s)$ was $\tilde{A}_2 s^{-2}$. The values of the fitted parameters are given in Table I; they clearly are quite different from those of the true potential. The resulting $\tilde{V}(s)$ is shown in Fig. 6, where it is compared with the actual potential used to generate the Monte Carlo data. What is important, however, is that the fitted and true potentials are close over the range in s corresponding to significantly nonzero $P(s)$ — in this case, $0.5 \le s \le 1.5$.

The phenomenological TWD (Fig. 5) derived from these fitted parameters is in good agreement with the Monte Carlo TWD and is very difficult to distinguish from the TWD derived from the true potential via Eq. (33). This result underscores the sensitivity of the process of extracting $\tilde{V}(s)$ and the necessity of very good statistics in experimental TWDs [38] and a good idea of the functional form of $\tilde{V}(s)$.

For this reason, we strongly recommend making a simultaneous fit of $V(L)$ to experimental TWDs from *several* different misorientations, and preferably from *several* different temperatures. We are currently applying this approach to Cu surfaces vicinal to the (001) plane [37]. We have selected 10 experimental TWDs to be fitted, with mean step separations ranging from $5.44a$ to $9.53a$, where the lattice constant $a = 0.255$ nm, and with temperatures ranging from 285 K to 360 K. Our preliminary studies [39] show that even with experimental data of good quality, the extraction of real potentials is not a trivial matter.

Using all 10 experimental TWDs, we were able to obtain good agreement between fitted TWDs and experimental TWDs; two examples are shown in Fig. 7. The corresponding interaction potential is shown in Fig. 8; clearly, it deviates markedly from Eq. (1). The irregularities in $V(L)$ make it plausible that a coexistence exists between two step widths, which would result in a diverging compressibility. This is supported by the fact that the experimental TWDs are fitted with $U(L) \propto L$ than with $U(L) \propto L^2$; furthermore, the linear form of $U(L)$ would lead to "fatter" tails, as were observed in Ref. 25.

Although these results show internal consistency, the fitted interaction potential is markedly different from potentials derived from simulations of surface relaxation using an empirical many-body potential [40, 41, 42, 43], which are in reasonable agreement with Eq. (1). We believe that our interaction potentials are "over-fitted" to the experimental data, with the irregularities of the $V(L)$ being too strongly influenced by statistical noise in our experimental data. This is not really surprising, because $V(L)$ depends quite sensitively on $P(L)$.

A similar problem [44, 45] occurs in determining embedding functions for the Embedded Atom Model from experimental data; if too many parameters are fitted, the resulting embedding functions of course can fit the supplied experimental data, but they give *worse* agreement with experimental data not included in the fitting process. The recommended remedy [44, 45] is to divide the available data into two groups, one of which is used to perform the fits, and the other of which is used to test the robustness of the fits.

Presumably, the same remedy will work in our case. However, a more complete treatment of the problem, including estimates of the uncertainties of fitted functions, is deferred to a later paper [37].

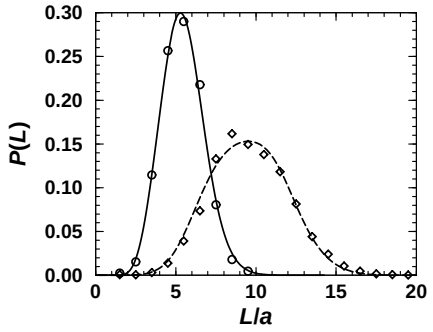

FIG. 7: Two experimental TWDs for Cu surfaces vicinal to the (001) plane. The circles are experimental data courtesy of M. Giesen, and the diamonds are experimental data courtesy of R. van Gastel. Both experiments were at 295 K. The corresponding fits were made by solving Eq. (33) with the potential shown in Fig. 8 and $U(L) \propto L$.

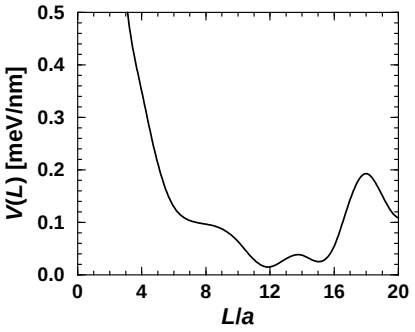

FIG. 8: The step-step interaction potential for for Cu surfaces vicinal to the (001) plane, as determined from fits to ten experimental TWDs like those shown in Fig. 7. This potential is in good agreement with experimental TWDs, but it has probably been "over-fitted."

V. CONCLUSIONS

We have seen that the generalized Wigner distribution can be derived from a Schrödinger equation somewhat in the spirit of the Gruber-Mullins approximation, and that straightforward extensions of this method work for general step-step interactions.

In Sec. II we saw that the generalized Wigner distribution can be derived exactly from the two-fermion Calogero model [8]. This, in turn, can be justified from a phenomenological model in which the force on two adjacent fermions is derived from the position-dependent pressure exerted by other fermions confined in a box, the size of which is presumably related to the correlation length in the x-direction. It is worth noting that the "entropic repulsion" is handled implicitly by the uncertainty

principle in the quantum mapping, so we need explicitly consider only the energetic interactions.

Nothing in this phenomenological picture requires the step-step interaction to be given by Eq. (8), and in Sec. III we demonstrate numerally that for very general step-step interactions the phenomenological picture yields TWDs in excellent agreement with numerical simulations of the TSK model. This success is particularly impressive when a coexistence between two well-defined step widths occurs, as can happen when steps bunch [36]. Under this circumstance the compressibility diverges, which causes the tail of the TWD to decay exponentially with L rather than exponentially with L^2, as it does in the case of the generalized Wigner distribution. This phenomenon could explain the curious slowly decaying tails of TWDs mentioned in Ref. 25.

Since exact solutions are available for both equations in the important case in which $\tilde{V}(s)$ is given by Eq. (8), it is possible to find not only the TWD but also, using the methods of Ref. 32, an improved estimate of step wandering. This will be undertaken in a separate paper.

Finally, although we have addressed this work primarily to its surface science applications, it may be of interest to research in random matrix theory as well. The Calogero-Sutherland model with $\tilde{A} = -1/4$, 0, or 2 corresponds to random matrices with specific symmetries, and attempts to interpolate between them have simply varied the fraction of matrices belonging to each symmetry in the ensemble of random matrices. It is far from clear, however, what relation the Calogero-Sutherland model with more general values of $\tilde{A}$ or our treatment of it has to such mixed ensembles.

Acknowledgment

Work was supported by the NSF-MRSEC at U. of Maryland Grant No. NSF-DMR 00-80008 and benefited from interactions with J. D. Weeks, M. Uwaha, and E. D. Williams. The authors also thank M. Haftel for useful discussions on numerical methods, and M. Giesen and R. van Gastel for experimental TWDs for copper surfaces and helpful comments.

[1] E. E. Gruber and W. W. Mullins, J. Phys. Chem. Solids **28**, 875 (1967).
[2] N. C. Bartelt, T. L. Einstein, and E. D. Williams, Surf. Sci. **240**, L591 (1990).
[3] O. Pierre-Louis and C. Misbah, Phys. Rev. B **58**, 2265 (1998).
[4] T. Ihle, C. Misbah, and O. Pierre-Louis, Phys. Rev. B **58**, 2289 (1998).
[5] L. Masson, L. Barbier, J. Cousty, and B. Salanon, Surf. Sci. **317**, L1115 (1994).
[6] L. Barbier, L. Masson, J. Cousty, and B. Salanon, Surf. Sci. **345**, 197 (1996).
[7] E. L. Goff, L. Barbier, L. Masson, and B. Salanon, Surf. Sci. **432**, 139 (1999).
[8] F. Calogero, J. Math. Phys. **10**, 2191, 2197 (1969).
[9] B. Sutherland, J. Math. Phys. **12**, 246 (1971); Phys. Rev. A **4**, 2019 (1971).
[10] T. Dittrich, P. Hänggi, G.-L. Ingold, B. Kramer, G. Schön, and W. Zwerger, *Quantum Transport and Dissipation* (Wiley-VCH, New York, 1998), pp. 54–56.
[11] M. L. Mehta, *Random Matrices*, 2nd ed. (Academic, New York, 1991).
[12] F. Haake, *Quantum Signatures of Chaos* (Springer, Berlin, 1991).
[13] T. Guhr, A. Müller-Groeling, and H. A. Weidenmüller, Phys. Rep. **299**, 189 (1998).
[14] T. A. Brody, Lett. Nuovo Cimento **7**, 482 (1973).
[15] M. V. Berry and M. Robnik, J. Phys. A **17**, 2413 (1984).
[16] H. Hasegawa, H. J. Mikeska, and H. Fram, Phys. Rev. A **38**, 395 (1988).
[17] F. M. Izrailev, J. Phys. A **22**, 865 (1989).
[18] G. Casati, F. M. Izrailev, and L. Molinari, J. Phys. A **24**, 4755 (1991).
[19] A. Y. Abdul-Magd, J. Phys. A **29**, 1 (1996).
[20] V. K. B. Kota and S. Sumedha, Phys. Rev. E **60**, 3405 (1999).
[21] T. L. Einstein and O. Pierre-Louis, Surf. Sci. **424**, L299 (1999).
[22] Cf., e.g., M. Lässig, Phys. Rev. Lett. **77**, 526 (1996).
[23] T. L. Einstein, H. L. Richards, S. D. Cohen, and O. Pierre-Louis, Surf. Sci. **493**, 62 (2001).
[24] Hailu Gebremariam, S. D. Cohen, H. L. Richards, and T. L. Einstein, Phys. Rev. B **69**, 125404 (2004).
[25] M. Giesen and T. L. Einstein, Surf. Sci. **449**, 191 (2000).
[26] P. J. Forrester, Nucl. Phys. B **388**, 671 (1992).
[27] F. D. M. Haldane, in *Correlation Effects in Low-Dimensional Electronic Systems*, edited by A. Okiji and N. Kawakami (Springer, Berlin, 1994), p. 3.
[28] Z. N. C. Ha, Nucl. Phys. B **435**, 604 (1995).
[29] I. I. Gol'dman and V. D. Krivchenkov, *Problems in Quantum Mechanics* (Dover, New York, 1993), pp. 52–53.
[30] I.S. Gradsteyn and I.M. Ryzhik, *Table of Integrals, Series, and Products*, (Academic Press, San Diego, 1980) §9.21; http://mathworld.wolfram.com/ConfluentHypergeometricFunctionoftheFirstKind.html
[31] This is a rough argument which is really intended to show only two things: (1) the pressure $\mathcal{P}$ on a fermion is a function of the position of the fermion, and (2) the second terms in Eqs. (19) and (21) are proportional to κ^{-1}. To the extent that $\mathcal{V}$ has a physical meaning, it should be related to the correlation length in the x-direction, but we have not attempted a careful study of this relationship.
[32] N. C. Bartelt, T. L. Einstein, and E. D. Williams, Surf. Sci. **276**, 308 (1992).
[33] N. Akutsu, Y. Akutsku, and T. Yamamoto, Prog. Theor. Phys. **105**, 323 (2001); Surf. Sci. **493**, 475 (2001) [cond-mat/0011210].
[34] W. W. Pai, J. S. Ozcomert, N. C. Bartelt, T. L. Einstein, and J. E. Reutt-Robey, Surf. Sci. **307-309**, 747 (1994)

obtained reasonable agreement with data for Ag(110) using such a potential with an L^{-2} rather than $L^{-3/2}$ decay envelope for the oscillatory term.

[35] T. L. Einstein, in *Physical Structure of Solid Surfaces*, edited by W. N. Unertl (Elsevier, Amsterdam, 1996), Vol. 1, p. 577; Per Hyldgaard and T. L. Einstein, J. Crystal Growth (in press) [cond-mat/0408645].

[36] V. B. Shenoy, S. Zhang, and W. F. Saam, Phys. Rev. Lett. **81**, 3475 (1998); Surf. Sci. **467**, 58 (2000).

[37] H. L. Richards, J. A. Yancey, T. L. Einstein, M. Giesen, and R. van Gastel, in preparation (unpublished).

[38] H. L. Richards, S. D. Cohen, T. L. Einstein, and M. Giesen, Surf. Sci. **453**, 59 (2000).

[39] J. A. Yancey, master's thesis, Texas A & M University–Commerce (2004), unpublished.

[40] F. Raouafi, C. Barreteau, M. C. Desjonquères, and D. Spanjaard, Surf. Sci. **482-485**, 1413 (2001); **505**, 183 (2002).

[41] C. Barreteau, F. Raouafi, M. C. Desjonquères, and D. Spanjaard, Surf. Sci. **519**, 15 (2002).

[42] M. C. Desjonquères, D. Spanjaard, C. Barreteau, and F. Raouafi, Phys. Rev. Lett. **88**, 056104 (2002).

[43] F. Raouafi, C. Barreteau, D. Spanjaard, and M. C. Desjonquères, Phys. Rev. B **66**, 045410 (2002).

[44] I. J. Robertson, V. Heine, and M. C. Payne, Phys. Rev. Lett. **70**, 1944 (1993).

[45] Y. Mishin, D. Farkas, M. J. Mehl, and D. A. Papaconstantopoulos, Phys. Rev. B **59**, 3393 (1999).